ACS Infectious Diseases

Article

pubs.acs.org/journal/aidcbc

Flexible vs Rigid Epitope Conformations for Diagnostic- and Vaccine-Oriented Applications: Novel Insights from the *Burkholderia pseudomallei* BPSL2765 Pal3 Epitope

Alessandro Gori,[*,†] Claudio Peri,[†] Giacomo Quilici,[‡] Arnone Nithichanon,[§] Davide Gaudesi,[‡] Renato Longhi,[†] Louise Gourlay,[∥] Martino Bolognesi,[∥,⊥] Ganjana Lertmemongkolchai,[§] Giovanna Musco,[‡] and Giorgio Colombo[*,†]

[†]Istituto di Chimica del Riconoscimento Molecolare, Consiglio Nazionale delle Ricerche, Via Mario Bianco, 9, 20131, Milan, Italy

[‡]Biomolecular NMR Laboratory, Division of Genetics and Cell Biology, S. Raffaele Scientific Institute, 20132 Milan, Italy

[§]Center for Research and Development of Medical Diagnostic Laboratories (CMDL), Faculty of Associated Medical Sciences, Khon Kaen University, 40002, Khon Kaen, Thailand

[∥]Department of Biosciences, University of Milan, 20133, Milan, Italy

[⊥]CNR-IBF and Cimaina, c/o Department of Biosciences, University of Milan, 20133, Milan, Italy

Supporting Information

ABSTRACT: Peptides seldom retain stable conformations if separated from their native protein structure. In an immunological context, this potentially affects the development of selective peptide-based bioprobes and, from a vaccine perspective, poses inherent limits in the elicitation of cross-reactive antibodies by candidate epitopes. Here, a 1,4-disubstituted-1,2,3-triazole-mediated stapling strategy was used to stabilize the native α-helical fold of the Pal3 peptidic epitope from the protein antigen Pal_{Bp} (BPSL2765) from *Burkholderia pseudomallei*, the etiological agent of melioidosis. Whereas Pal3 shows no propensity to fold outside its native protein context, the engineered peptide (Pal3H) forms a stable α-helix, as assessed by MD, NMR, and CD structural analyses. Importantly, Pal3H shows an enhanced ability to discriminate between melioidosis patient subclasses in immune sera reactivity tests, demonstrating the potential of the stapled peptide for diagnostic purposes. With regard to antibody elicitation and related bactericidal activities, the linear peptide is shown to elicit a higher response. On these bases, we critically discuss the implications of epitope structure engineering for diagnostic- and vaccine-oriented applications.

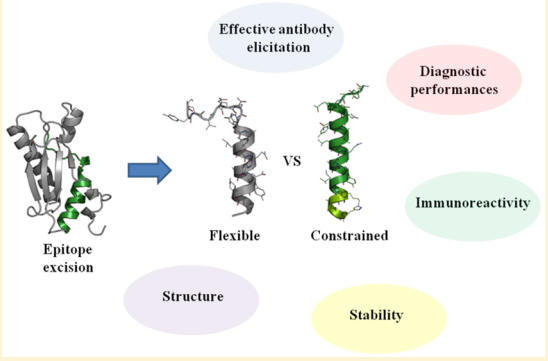

KEYWORDS: *epitope engineering, peptide stapling, melioidosis, structural vaccinology, bioprobes, antigen design*

Pathogen resistance to many classes of therapeutics, in particular antibiotics, represents an ever increasing threat to human health and poses major challenges for effective management of infections.[1,2] In this context, vaccination plays a pivotal role in disease prevention and treatment.[3,4] In parallel, the importance of early diagnosis in efficient disease management is driving the demand for new, reliable diagnostic tools.[5−7]

Recent years have witnessed a growing interest toward the exploitation of peptides in the diagnostic and vaccine fields, mainly due to their ease of synthesis and manipulation, which can potentially overcome practical and regulatory limitations associated with the traditional use of attenuated or inactivated microorganisms for vaccination purposes.[8] In addition, the demonstrated advantages of using peptides as diagnostic tools and biomarkers, particularly the possibility to include post-translational modifications in a controlled fashion, has further contributed to increase their popularity in the immunological field.[9]

While very promising, the exploitation of peptides in vaccine development has so far encountered only limited success.[10] Multiple reasons account for such results, in particular, their intrinsic poor immunogenicity and inherent instability in biological media due to protease-mediated degradation.[11] Moreover, while the activation of the T-cell-mediated immune response is a conformation-independent process, the role of epitope conformation in eliciting neutralizing antibodies is proposed to be important for selective cross-reactivity toward the native antigen.[12] Indeed, theoretically, antibodies generated against an epitope that closely resembles its counterpart within the native antigen have a higher probability to cross-react with it. Unfortunately, short peptides seldom retain their original

Received: October 5, 2015
Published: December 23, 2015

DOI: 10.1021/acsinfecdis.5b00118
ACS Infect. Dis. 2016, 2, 221−230

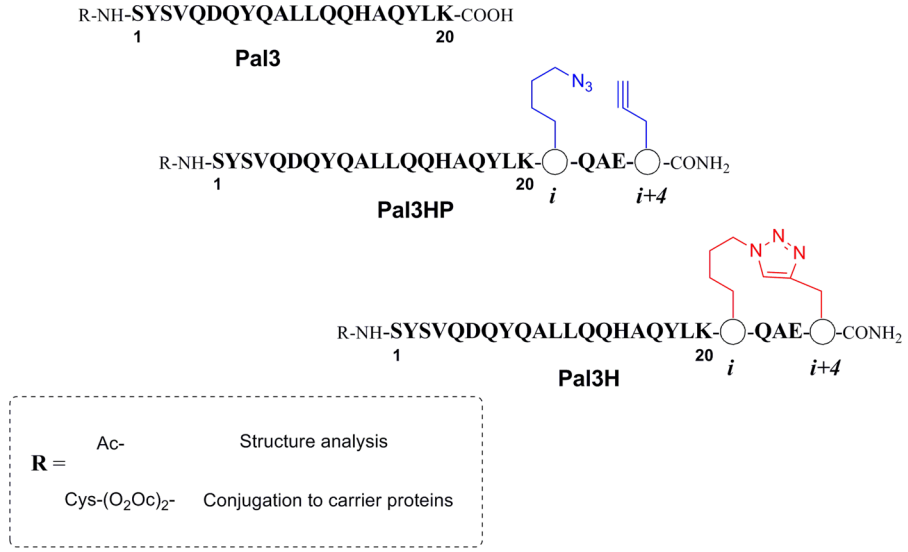

Figure 1. Linear sequences and schematic representation of Pal3, Pal3HP, and Pal3H. Peptides were produced in acetylated form for structural analyses and contained a PEG spacer (O_2Oc) and a N-terminal cysteine for conjugation to carrier proteins. An unrelated *B pseudomallei* peptide sequence (VSNKYFSNIHW[Lys-N3]QAE[Prg], UnP) was used as a negative control.

conformations when taken out of their native context. For such reasons, the successful development of effective peptide vaccines has proven extremely challenging so far. Likewise, the use of unstructured peptide ligands may lead to heterogeneous presentation of the peptide-bioprobe in diagnostic assays, potentially undermining their discrimination performances.[13] Structurally constrained peptides are therefore appealing to enable optimal functionality of the peptidic probe with respect to a ligand−target interaction.

Conformational restriction of free peptides in the immunological field has been addressed using different approaches. For instance, grafting of functional motifs onto protein scaffolds has been elegantly exploited to replicate the antigenic surface recognized by target antibodies.[14−16] Importantly, this approach has the potential to reproduce complex, discontinuous epitopes. Similarly, antigen surface mimicry has been achieved by generating fully synthetic constructs through cyclization onto scaffolds of otherwise linear peptide epitopes, which was shown to enable the functional reconstruction of discontinuous epitopes.[17−19] Additionally, cyclization of single linear peptides has proven successful for the generation of neutralizing antibodies in cases where linear precursors failed.[20] However, epitope engineering in conformationally-locked derivatives has been shown to have variable success. The Keller and the MacDonald groups, for instance, reported on the ineffective application of epitope conformational engineering to elicit neutralizing antibodies, despite the fact that an improvement in epitope antigenicity was obtained.[21,22] This observation suggests that the relationship between epitope conformation, epitope reactivity, and the ability to generate an effective response should to be cautiously pondered, especially with regard to a complex system such as the immune response.

Peptide stapling, that is the introduction of structural constraints that force the peptide to adopt a defined conformation, has been shown to positively affect the activity and stability profiles of peptides in a number of drug development reports.[23] Tightly folded peptides of rigid structure often display remarkable and, in some cases, astonishing resistance to proteolysis.[24] Such stabilization could either result from a structural effect, that is limited exposure to protease cleavage sites, or from active protection by the staple. Epitope structure engineering by introducing covalent staples has been recently proposed as a viable way to improve vaccine feasibility of peptide candidates.[25] Accordingly, stabilizing specific peptide conformations through chemical scaffolds helps to preorganize atom patches along the backbone that recapitulate the original antigenic structure, in order to potentially trigger a selective antibody-mediated response. Moreover, tightening the overall structure, along with "active shielding" by the staple, limits the exposure of protease cleavage sites, resulting in a generally improved metabolic stability.[26]

In a recent report, we identified an immunoreactive epitope from the peptidoglycan-associated lipoprotein BPSL2765 ($\mathbf{Pal_{Bp}}$), from the pathogen *B. pseudomallei*, the etiological agent of melioidosis that stimulated the production of opsonizing antibodies.[27] The reported epitope (**Pal3**) is a promising lead candidate as a prospective vaccine component and could also have applications in melioidosis diagnosis. Intriguingly, this 20 amino acid peptide is almost completely α-helical within the full antigen. In the present work, starting from the observation that **Pal3** does not maintain the original α-helical conformation as a free peptide (circular dichroism (CD) analysis), we set out to evaluate the effect of structural stabilization on **Pal3** antigenic properties; we thus produced an artificially folded epitope and compared its properties with those of the original, linear **Pal3** peptide. To this end, we envisioned the use of a stapling strategy to stabilize the **Pal3** native α-helical structure. We first selected an extra-sequence oligopeptidic triazole-bridged macrocyclic scaffold as a suitable helix-stabilizing template; we confirmed α-helical stabilization by performing synthesis and detailed structural analysis of the engineered epitope **Pal3H** (MD, CD, and NMR analysis). We then investigated the influence of structural stabilization on the immunoreactivity of **Pal3** against sera from diverse melioidosis patient subclasses. In this context, **Pal3H** showed superior performances with respect to the linear **Pal3** peptide, supporting a potential application in diagnostics. It should be noted here that no reliable and efficient molecular diagnostic test for *B. pseudomallei* infection exists to date. We also assessed

DOI: 10.1021/acsinfecdis.5b00118
ACS Infect. Dis. 2016, 2, 221−230

the ability of **Pal3** versus **Pal3H** to elicit antibodies that recognize and kill the bacteria *in vitro*, and showed that conformational flexibility can be beneficial for the elicitation of an effective Ab-mediated response. In parallel, we performed *in vitro* studies on the stability of the stapled peptide in human plasma, in comparison with the unfolded precursor. Our results show that the engineered peptide **Pal3H** has a vastly enhanced plasma half-life that might be reflected by an improved metabolic stability *in vivo*. Finally, we discuss the roles and implications of epitope structural engineering and conformational selection for potential diagnostic and vaccine-oriented applications.

RESULTS AND DISCUSSION

Design and synthesis. While hydrocarbon stapling via ring closing metathesis (RCM) is growing in popularity, several other approaches are also viable to promote peptide folding, such as thioether cross-links, disulfide bonds, and triazole bridges.[28] In particular, the use of a triazole scaffold in the synthesis of peptidomimetics is well established thanks to its ready synthetic accessibility, combined with its proven stability in biological media.[29,30] On these bases, we selected a triazole scaffold stapling strategy to enable **Pal3** α-helical stabilization (Figure 1). To avoid any possible interference of the staple with the **Pal3** epitope region, we envisioned the use of an extra-sequence rigid oligopeptidic scaffold as folding nucleator to assist the formation and stabilization of the native α-helix. Propargylglycine (Prg) and azidolysine (Lys-N_3) were selected as the intramolecular (side-chain) cyclization partners. Indeed, previously reported data suggested an optimal size of 5 or 6 methylene groups in the triazole bridge to obtain a regular ordered structure.[31,32]

The **Pal3H** linear precursor (**Pal3HP,** i.e before ring closure) was assembled on a Rink Amide PEG AM resin by a fully automated microwave-assisted Fmoc-SPPS protocol.[33] Prg and Lys-N_3 were incorporated at positions p1 and p5 of the oligopeptidic insert, to allow subsequent intramolecular macrocyclization. Copper-catalyzed-azide−alkyne-cycloaddition (CuAAC) was performed on **Pal3HP** by forming *in situ* the Cu^I catalyst using $CuSO_4$/ ascorbic acid, to finally generate the 1,4-disubstituted-1,2,3-triazole staple.[34,35] The reaction proceeded smoothly to give full conversion of the linear precursor to the cyclized product (i.e., **Pal3H**; RP-HPLC monitoring, Figure S1). Triazole formation was assessed by reduction with DTT on both the linear precursor and the cyclic clicked product.[36] **Pal3** synthesis was previously reported.[27] **Pal3** and **Pal3H** were produced as N-terminally acetylated forms for structural analyses, while sequence extension with short-chain PEG spacers (O_2Oc) bearing a terminal cysteine was used to allow subsequent conjugation to human serum albumin (HSA, for ELISA spot) and keyhole lympet hemocyanin (KLH, for rabbit immunization) via maleimide-mediated conjugation.[37] Antisera obtained upon rabbit immunization were purified by affinity chromatography (See Methods).

Structural analysis. The initial assessment of the structural properties of **Pal3** vs **Pal3H** was carried out by Molecular Dynamics simulations (MD) to gain insights into the structural and dynamic properties of epitopes **Pal3** and **Pal3H**.[38−40] Analysis of the time-evolution of secondary structures during the MD trajectories, confirmed the inability of **Pal3** to maintain the α-helical conformation in its free form (Figure S4). In contrast, the constrained peptide **Pal3H** showed strong α-helical propensity in all three replicas (Figure S4). This first evaluation was then followed by CD analysis. **Pal3** showed no well-defined structured pattern and, in particular, no characteristic α-helical feature in the CD spectra (Figure 2). On the contrary, **Pal3H** displayed a remarkable propensity to fold into a α-helical structure, as revealed by spectral minima in the 222 and 208 nm regions, distinctive of helical conformations (Figure 2), corroborating MD calculations. To assess the stability of the α-helical **Pal3H** structure, we recorded CD spectra at variable temperatures (Figure S5). We observed that **Pal3H** retains a significant degree of helicity even at high temperatures (25% helicity at 60 °C), and that the α-helical fold is promptly and fully regained after complete thermal denaturation. Overall, CD analyses highlighted a significant effect of the triazole staple in inducing a stable α-helical conformation.

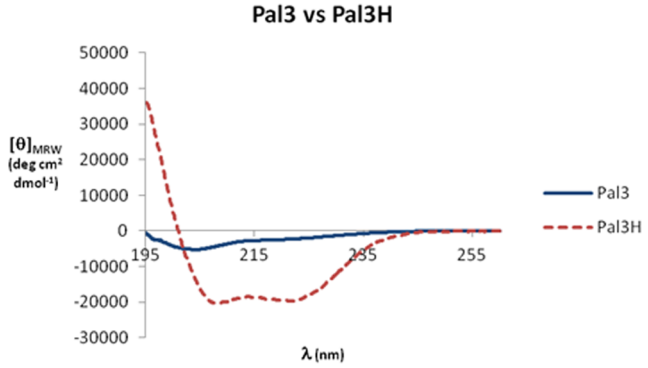

Figure 2. Circular dichroism spectra comparisons between Pal3 and Pal3H (20 °C); Pal3 displays the typical CD profile of an unfolded protein, whereas Pal3H displays the classical α-helical spectrum profile.

Next, to generate a reliable structural model of **Pal3H** and to verify that the α-helical structure matches the respective domain in the full Pal_{Bp} protein antigen, we performed NMR analysis. Canonical α-helix NOE-crosspeaks (NH_i-NH_{i+1}; Ha_i-NH_{i+3}, Ha_i-Hb_{i+3}) were observed for the epitope region corresponding to Pal3 (residues 3−22; Figure 3 and Figure S6). Moreover, secondary chemical shifts calculated for the Hα protons confirmed the presence of an α-helix in this region. NOE derived distances were then used to drive computational refinement to generate the whole **Pal3H** structure, including the oligopeptidic triazole scaffold used to stabilize the α-helical conformation. The resulting calculated structures revealed a close structural fit between **Pal3H** and the corresponding α-helical region within the native Pal_{Bp} antigen (RMSD 0.78 Å; Figure 4A).

Overall, from our comprehensive structural analyses, we ascertained that our stapling strategy successfully stabilized the native α-helical fold of the **Pal3** epitope region; we then proceeded to perform functional evaluations on **Pal3H**.

***In vitro* stability of Pal3 vs Pal3H in human plasma.** Stability assays in human plasma comparing **Pal3**, **Pal3H** and **Pal3HP** were performed to assess the potential of structure-stabilizing stapling on vaccine-oriented epitope candidates. Not surprisingly, the **Pal3** peptide was readily and almost completely degraded upon incubation in plasma at 37 °C ($t_{1/2}$ < 1 h by HPLC monitoring, see Figure S8). The linear **Pal3HP** precursor also displayed a similar profile (not shown). On the contrary, stapled **Pal3H** showed significantly enhanced plasma stability; a non-negligible amount of residual peptide was indeed still detectable after 24 h of incubation (Figure S9).

DOI: 10.1021/acsinfecdis.5b00118
ACS Infect. Dis. 2016, 2, 221−230

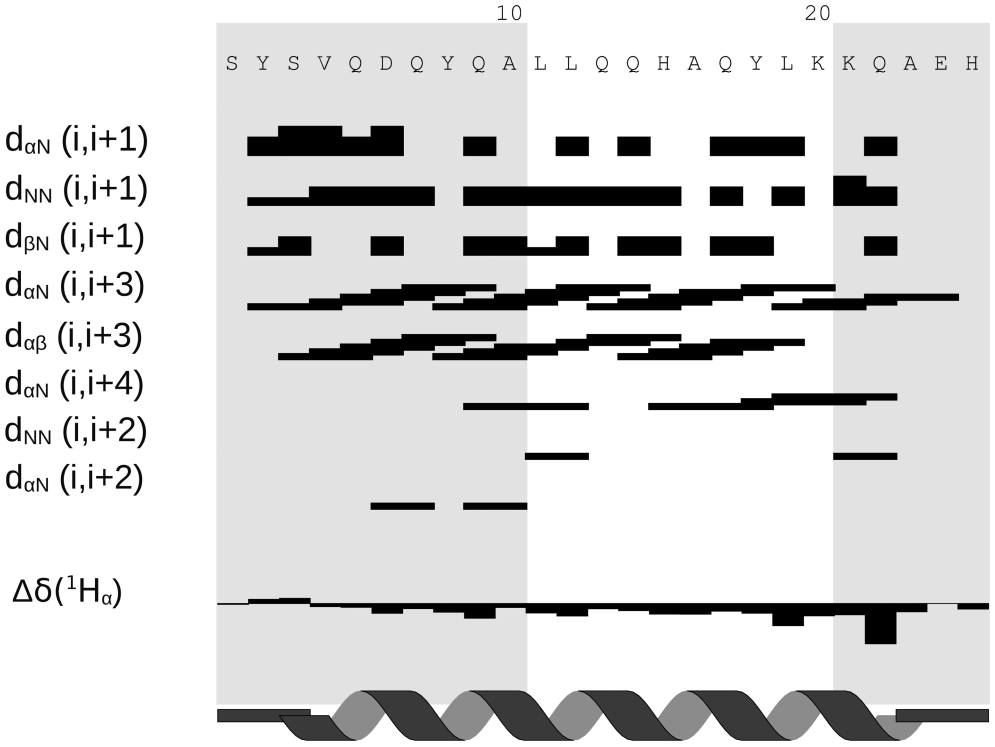

Figure 3. Schematic representation of NOE-crosspeaks (d) observed between amino acid (i) and (i + n; n = 1, 2, 3, 4), whereby the indexes α, β, and N indicate Hα, Hβ, and HN protons, respectively; ΔH_α corresponds to the Hα secondary chemical shift calculated with respect to the random coil values.

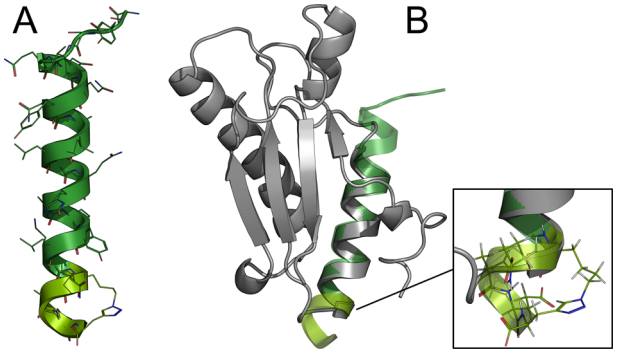

Figure 4. (A) Calculated structure for Pal3H using a combination of NMR NOE restraints and computational refinement. The oligopeptidic triazole scaffold is depicted in pale green. (B) Superposition of peptide Pal3H (green) with the native Pal3 sequence, as annotated in the high-resolution crystal structure of recombinant Pal_{Bp} (PDB ID 4B5C).

Overall, from a stability point of view, the potential of **Pal3H** as a vaccine candidate appears to be superior to that of the unstapled peptide.

Pal3 vs Pal3H immunoreactivity to human plasma antibodies. **Pal3** and **Pal3H** peptides were directly compared in antibody recognition experiments (Figure 5), probing with plasma samples collected from healthy seronegative (S−), healthy seropositive (S+), and recovered (R) melioidosis patient groups, by indirect ELISA tests (Figure 5A). The recombinant Pal_{Bp} protein antigen was used as a positive control. In agreement with previous reports, **Pal3** was confirmed to be a highly immunoreactive region of Pal_{Bp}. In particular, the level of reactive antibodies against the **Pal3** epitope was increased in recovered patients, while no discrimination was evident between the S+ and S- healthy groups. Importantly, compared to **Pal3**, **Pal3H** was more reactive against antibodies from the S+ group and, to a greater extent, in the R group. Such results imply improved discrimination properties of Pal3H (Figure 5B) and demonstrates its potential in diagnostic-oriented applications that is severely lacking for melioidosis.[41]

To investigate whether **Pal3H** recognition by human IgG is structure-dependent and whether extra-sequence amino acids are involved in the interaction, we tested the immunoreactivity of **Pal3HP** (the **Pal3H** linear precursor) toward plasma samples from the S+ and R groups (Figure 5C). Notably, **Pal3HP** showed a remarkably lower reactivity, relative to **Pal3H**, suggesting that epitope conformation may indeed play a significant role in the recognition by the antibodies from patients that had previously been exposed to *B. pseudomallei*, and that additional amino acids, introduced to allow intramolecular cyclization, are not beneficial for antibody recognition, at least in their linear form. The "inertness" of the triazole cyclic scaffold was later confirmed (see next section). Furthermore, to critically assess the roles of peptide conformational rigidity vs flexibility in eliciting cross-reactive antibodies, polyclonal anti-Pal3 and anti Pal3H antibodies were raised in rabbits for further evaluation.

Rabbit antisera recognition experiments. **Pal3** and **Pal3H** were conjugated to the keyhole limpet hemocyanin (KLH) carrier protein to immunize rabbits according to established protocols (See Methods). Antisera were then collected and purified by affinity chromatography upon binding by immobilized peptides on a sepharose support (See Methods). The antibodies isolated from **Pal3** or **Pal3H** antisera were then screened for their reactivity against **Pal3**, **Pal3H**, **Pal3HP**, and an unrelated peptide containing the oligopeptidic

DOI: 10.1021/acsinfecdis.5b00118
ACS Infect. Dis. 2016, 2, 221−230

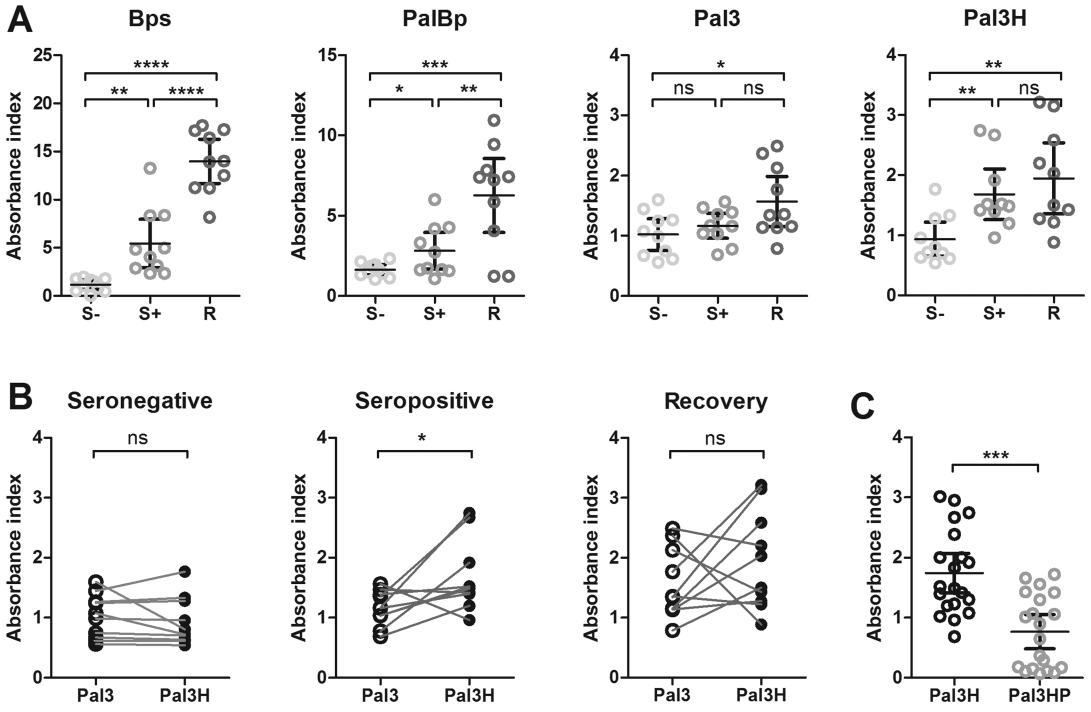

Figure 5. Immunoreactivity of recombinant Pal_{Bp} and peptides against human IgG in plasma. The level of human IgG in plasma against *B. pseudomallei* K96243 crude extract (Bps); recombinant Pal_{Bp}, Pal3; and Pal3H from seronegative (S−), seropositive (S+), and recovered (R) individuals (A). Comparison of the level of human antibody (IgG) recognition to Pal3 vs Pal3H (B) and Pal3H vs Pal3HP (C) (S+ and R individuals). The statistical differences between sample groups were tested by using an unpaired *t* test applied for the results in panel A, while a paired *t* test was applied for the results in panels B and C: ns represents nonsignificant; *, $P < 0.05$; **, $P < 0.01$; ***, $P < 0.001$; and ****, $P < 0.0001$.

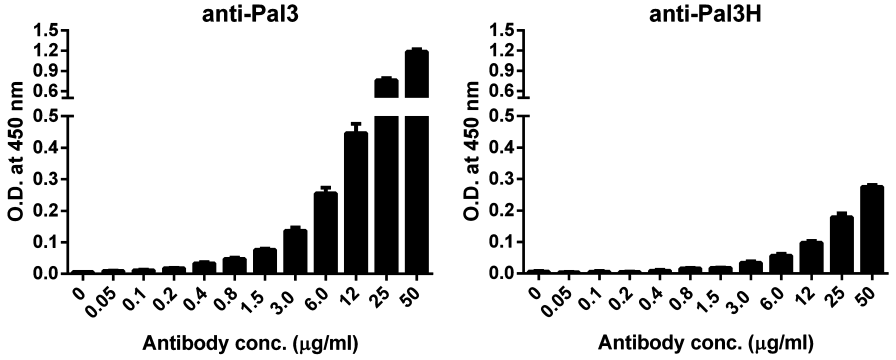

Figure 6. Purified anti-Pal3 and anti-Pal3H antibody (IgG) recognition of intact dead *B. pseudomallei* K96243.

triazole template used for α-helical stabilization, as a negative control (**UnP**) (Figure S10). As expected, neither anti-Pal3 nor anti-Pal3H antibodies showed recognition of **UnP**, suggesting that the antibody response is selective for the epitope sequence and not directed against the triazole staple, which may thus plays only a minor/negligible role in antibody elicitation. Both antisera showed a high degree of cross-reactivity (anti-Pal3 vs Pal3H and *vice versa*), as expected based on the sequence identity between **Pal3** and **Pal3H**, each antiserum being slightly more selective for its respective eliciting peptide. Moreover, despite the above-mentioned close sequence similarity, both antisera were less reactive toward the linear **Pal3HP** precursor, highlighting that the extra-sequence amino acids alone are not beneficial, but rather detrimental, to recognition.

Neutrophil opsonization killing experiments. Polyclonal anti-Pal3 and anti-Pal3H antibodies were further tested through enhancement experiments on neutrophil-mediated phagocytosis, oxidative burst and bacterial killing (OPK). We first compared the ability of anti-Pal3 and anti-Pal3H to recognize fixed intact *B. pseudomallei* bacterial cells (Bps). Both antisera were capable of recognition, the anti-Pal3 antibodies binding to a greater extent (by about a factor of 4) to intact Bps (Figure 6).

We then investigated the effect of various concentrations of anti-Pal3 and anti-Pal3H antibodies on phagocytosis and oxidative burst functions of purified human neutrophils, in response to live *B. pseudomallei*. Phagocytosis and oxidative burst (monitored by superoxide production) by neutrophils exposed to *B. pseudomallei* were significantly enhanced ($p < 0.05$) in the presence of anti-Pal3 antibodies. Accordingly, *in vitro* bacterial killing by neutrophils exposed to *B. pseudomallei* was also enhanced by the presence of anti-Pal3 antibodies. Anti-Pal3H antibodies elicited weaker but statistically significant effects (Figure 7). In summary, these experiments indicate that

DOI: 10.1021/acsinfecdis.5b00118
ACS Infect. Dis. 2016, 2, 221−230

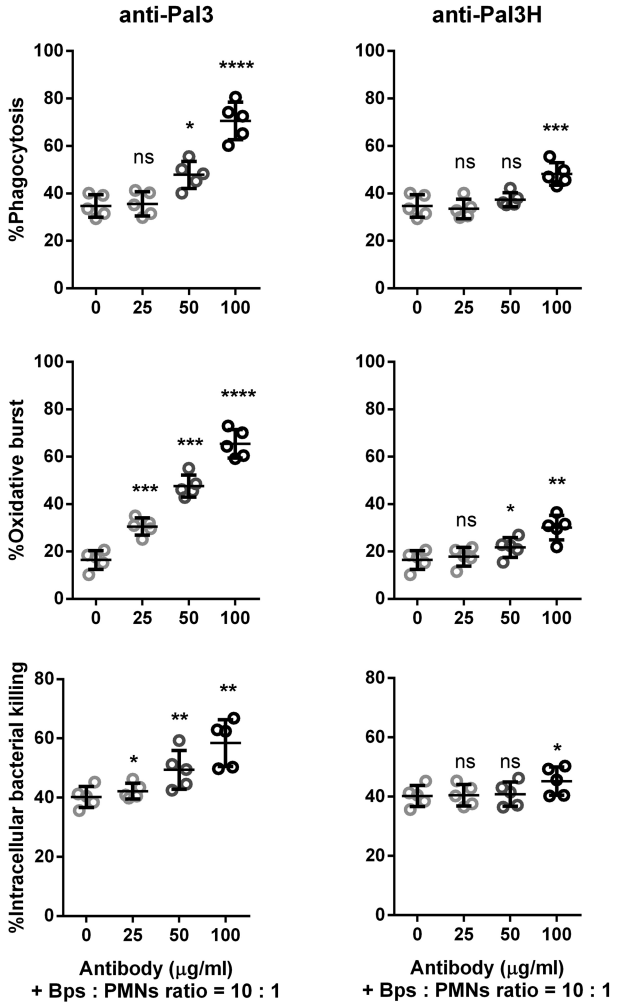

Figure 7. Purified anti-Pal3 and anti-Pal3H antibodies enhance phagocytosis, oxidative burst, and bacterial killing in human neutrophils. The statistical differences between sample groups were tested by using a paired *t* test: ns represents nonsignificant; *, $P < 0.05$; **, $P < 0.01$; ***, $P < 0.001$; and ****, $P < 0.0001$.

antibodies raised against both the designed epitopes are active in OPK; notably, anti-Pal3 antibodies outperform anti-Pal3H antibodies in recognizing and killing the bacteria.

DISCUSSION AND CONCLUSIONS

Melioidosis is a severe disease endemic in tropical and subtropical regions of the world, caused by *Burkholderia pseudomallei* infection. Melioidosis is difficult to diagnose (often misdiagnosed as tuberculosis), and *B. pseudomallei* infection is particularly hard to eradicate. Such considerations point to the development of new diagnostic tools and of vaccine candidates as an urgent matter.

Recent years have witnessed a growing interest toward an antigen-minimization approach exploring the use of peptides as vaccine candidates However, given the complexity of the processes driving the elicitation of an effective immune response, the minimization approach has so far encountered only limited fortune, with multiple reasons accounting for this.[10] For instance, focusing on the humoral response, antibodies affinity maturation may be dependent on additional protein antigen regions which are not included in excised peptide epitopes. In this case, the effectiveness of a single epitope in the elicitation of a good response could be intrinsically undermined by other factors than the lack of an appropriate structural context. Also, although a humoral response can even be generated against short unfolded peptide epitopes, the elicited antibodies may not be cross-reactive and effective against the native antigen due to the fact that they cannot bind to the epitope in the conformation(s) it populates in the context of the full-length protein.[42] The above rationale has driven the demand for chemical strategies to shape epitopes into the conformation they hold within the native cognate antigen context. In addition, constraining peptide conformations into a specific structure reduces the number of variable conformations that the sequence can assume, thus potentially increasing its discrimination performances in diagnostic assays by limiting heterogeneous bioprobe presentation.

Several cases of epitope engineering have been described, even though these approaches did not always prove successful in eliciting a protective response.[21,22] However, structural stabilization of isolated epitopes by means of macrocyclization, stapling, etc. is likely to improve the metabolic profile of engineered peptides, thereby enhancing their vaccine potential. Moreover, the impact of engineered/structured epitopes on the development of diagnostics remains largely unexplored. In this work, we critically assessed the role of **Pal3** epitope conformational stabilization in the development of immunoreactive probes for diagnostic purposes, and in view of its potential application as a prospective vaccine component.

We exploited a triazole stapling strategy to lock the **Pal3** epitope in a α-helical conformation, and compared its immunoreactivity, the ability to generate cross-reactive antibodies, and the stability in plasma of the unstructured (**Pal3**) vs the stabilized (**Pal3H**) epitope. To the best of our knowledge, this study represents one of the few cases in which such a comparison is performed, in particular with regard to the diagnostic application of a peptide stapling strategy. Overall, our results on the comparative analysis of the performances of the linear and structurally constrained epitopes provide new insight into the relationships between peptide sequence, conformation, and immunoreactivity properties. In particular, in our case, the data generated suggest a dual role for epitope conformational restriction. First, direct comparison of peptides' immunoreactivity revealed a clearly improved profile for the α-helical-stabilized **Pal3H** epitope, both in terms of response intensity and discrimination among the different melioidosis patient subclasses, highlighting a promising diagnostic potential. Notably, since the **Pal3** linear epitope had already shown increased immunoreactivity in comparison to the full-length Pal_{Bp} protein antigen, the improved immunoreactivity profile displayed by **Pal3H** is intriguing and in keeping with our finding that it is dependent on achievement of a stabilized α-helical structure. Second, as far as elicitation of a bactericidal antibody response is concerned, our results showed that anti-Pal3 antibodies outperform anti-Pal3H in functional OPK assays. Such results may be reconciled considering the ill-defined boundaries that characterize epitopes as binding sites, and taking into account how immunoglobulin−epitope interaction occurs at the molecular level. Indeed, epitopes are not discrete structural entities, but rather, it is often the case that the accessible surface of a protein domain harbors many overlapping epitopes, which in turn implies that the same antigen residues may be shared among different antibody binding regions.[12] Moreover, protein antigens are dynamic entities with different sets of conformers and, finally, induced fit

DOI: 10.1021/acsinfecdis.5b00118
ACS Infect. Dis. 2016, 2, 221−230

or mutual adaptation upon antigen−antibody interaction further contributes to increase the repertoire of antigen conformations antibodies can react with.

In this framework, it is possible to hypothesize that immunization with the structurally flexible **Pal3** elicits a pool of antibodies with broader cross-reactivity thanks to their ability to recognize several sets of conformations within the native antigen on the intact bacteria. Indeed, even in the context of the full-length protein, the **Pal3** epitope may be presented to B-cell response only in specific but transient conformations that are different from the conformation observed in the protein crystal structure. Anti-Pal3 immunoglobulins may select/induce one reactive conformation in the epitope by a conformational selection process, ultimately triggering the expansion of a large pool of broadly cross-reactive antibodies. On these bases, we speculate that mimicking the 3D structure of a certain antigen region observed in X-ray or NMR-based studies by means of structural constraints may not necessarily translate into an efficient B-cell response. The dynamic nature of protein antigens, and how this underlies their interaction with the immune system, should thus be critically considered. Indeed, our results show that the rigid structure of **Pal3H** (Figure S7) could induce a pool of antibodies less prone to undergo favorable mutual adaptation with the antigen in *ex vivo* experiments. In the case of **Pal3H**, the stabilized conformation may in fact not adopt that required to achieve cross-reactive immunogenicity, leading to a weaker response, consistent with previous findings.[10]

To summarize, our results suggest that modulating epitope flexibility could play a key role in developing molecules for immunological applications. Although flexibility may be more advantageous to generate a broader antibody-mediated response, more "selective recognition", induced by conformational stabilization of the restrained **Pal3H** epitope, played a favorable role in terms of diagnostic discrimination between the three patient groups. For melioidosis, for which no effective molecular diagnostic tools have been developed so far, the latter aspect is particularly important.

In conclusion, is restricting epitope conformation a double-edged sword? Overall, we speculate that in the absence of data on the conformation adopted by the epitope within the native antigen (that is required for eliciting cross-reactive antibodies), epitope optimization, based on 3D structural considerations alone, remains largely empirical. Our results emphasize the importance of epitope dynamics and conformational variability as a key factor for eliciting a cross-reactive antibody response. Interestingly, stable conformational preorganization/stabilization of peptide probes proved beneficial in view of diagnostic applications. Our results provide insight into the effects of structural variation on the immunological properties of specific peptide epitopes. Noteworthy, epitope shaping into defined conformations can be achieved by means of different approaches, including but not limited to covalent stapling. For instance, epitope motifs transplantation, a.k.a. grafting, into full protein antigens or carriers was shown in some reports to preserve native epitope structure.[14−16] This approach is certainly appealing toward vaccine-oriented applications, as epitope structural engineering can be associated with favorable adjuvating properties from the protein antigen/carrier the epitope is transplanted into (e.g., additional epitopes that drive B-cell expansion and maturation). Overall, it is worth underlining that the effectiveness of a conformational restriction strategy is likely case-dependent, and no dogmatic assumptions on its effects should be taken *a priori*. Most likely, fine-tuning the relationship between epitope structural and dynamic properties in a progressive epitope optimization process may be the key to deliver truly effective peptide-based immunogens.

METHODS

Peptide synthesis. All linear peptides were synthesized by stepwise microwave-assisted Fmoc-SPPS on a Biotage ALSTRA Initiator+ peptide synthesizer according to well-established protocols, and purified by preparative RP-HPLC. Linear Pal3H precursor underwent intramolecular cyclization by CuAAC using $CuSO_4$/ascorbic acid to generate *in situ* the Cu^I catalyst. Reactions proceeded smoothly to completion within 30 min. Peptides were then conjugated to carrier proteins for immunization purposes (KLH) or for ELISA (HSA) using SMCC bifunctional linker. Further experimental details are described in the Supporting Information.

Production and purification of anti-Pal3 and anti-Pal3H antibodies. Rabbit polyclonal antibodies were generated by Primm SRL, Milano, Italy. Antisera were purified by affinity against the peptides, chemically linked to cyanogen bromide activated sepharose (Sigma-Aldrich) following the manufacturer's instructions.

Circular dichroism measurements. CD spectra were acquired on a Jasco J-815 using a rectangular quartz cuvette (1 mm path length, Hellma). Each spectrum was averaged over 4 scans collected in 0.1 nm intervals with an average time of 0.5 s. Typical peptides concentrations were 20 μM. All samples have been prepared in 10 mM NaF, 20 mM NaH_2PO_4/Na_2HPO_4 buffer, pH 6.24. Spectra have been acquired at 20 °C. All the spectra were baseline corrected by subtracting buffer spectra, and the observed ellipticity was converted to mean residue weight ellipticity $[\theta]$/deg.cm^2.dmol^{-1}. The helical population was estimated from the measured mean residue weight ellipiticity at 222 nm assuming a value of $-39500 \times (1 - 2.57/n)$ (where n is the peptide length) for 100% helicity.[43]

Molecular dynamics. MD simulations were performed for peptides Pal3 and Pal3H with explicit solvent under NPT conditions. Three replica runs were set up for both the stapled peptide (Pal3H) and the control (Pal3), using the Molecular Dynamics software package AMBER 14[44] and the AMBER99SB force field. The production runs were carried out for 250 ns. The initial 3D structure of the staple was modeled with Maestro, from Schrödinger software, and treated according to the general amber force field (GAFF)[45] and BCC charge correction method.[46] The time evolution analysis of secondary structure was performed for each replica with DSSP[47,48] and AMBER 14 on 1K frames trajectories. The final reconstruction of Pal3H was calculated starting from the complete atomic coordinates of the epitope and the NOE distances of the staple as measured by NMR. A complete initial structure of the stapled peptide was modeled with Maestro and refined by the previously described MD protocol. In this case, NOE distances were integrated as distance restraints, while the epitope structure was kept rigid by constraints. The final structure was retrieved after a 500 ps equilibration.

NMR measurements. NMR experiments were performed at 298 K on a 600-MHz spectrometer (Bruker Avance 600 Ultra Shield TM Plus, Bruker BioSpin) equipped with a triple-resonance TCI cryoprobe with a z-shielded pulsed-field gradient coil. Data were processed with Topspin (v. 3.0) (Bruker Biospin) and analyzed with CCPN analysis 2.2

DOI: 10.1021/acsinfecdis.5b00118
ACS Infect. Dis. 2016, 2, 221−230

software.[49] Pal3H (1 mM) was dissolved in 20 mM NaH_2PO_4/Na_2HPO_4 buffer (pH 6.3), 150 mM NaCl. 2D TOCSY was acquired with 32 scans, 2048 × 512 complex points and 60 ms mixing time. 2D NOESY was acquired with 48 scans, 2048 × 512 complex points, mixing times of 100 and 200 ms. 2D NMR experiments were acquired both in H2O and D2O (100%). The ^{1}H chemical shifts of backbone and side chains resonances were assigned using the classical sequential assignment procedure.[50]

Human plasma stability. The stability of the peptides in human serum (Sigma-Aldrich) was measured by incubation of peptide samples at 37 °C (20 μM, triplicate). Aliquots were taken at predetermined intervals, quenched with 15% aqueous trichloroacetic acid to precipitate serum proteins and stored at 0 °C.[51] The samples were then centrifuged and the supernatant collected and stored at −20 °C until RP-HPLC analysis. Time-point aliquots were injected and the amount of intact peptide remaining was determined by integration at 210 nm.

Immunoreactivity screening. Human antibodies (IgG) recognition to protein/peptide was determined by indirect ELISA as previously described.[27] Briefly, 96 well ELISA plates (Nunc Maxisorp) were precoated overnight with 1 ug/mL of *B. pseudomallei* K96243 crude extract (crude Bps), 10 ug/mL of Pal_{Bp} protein or human serum albumin (HSA) conjugated peptides. After blocking with 10% fetal bovine serum (BSA) in phosphate buffer saline (PBS), 1:300 diluted plasma samples were probed in duplicate. Antibodies binding to coated antigens were detected by using biotinylated rabbit antihuman IgG with horse radish peroxidase conjugated streptavidin (BD biosciences). Immunoreactivity was detected and represented as absorbance index of individual samples = $(O.D._{test} - O.D._{uncoated})/O.D._{uncoated}$.

Opsonization and oxidative burst activities in human polymorphonuclear cells (PMNs). The whole procedure was carried out as previously described.[27] Briefly, FITC-labeled intact dead *B. pseudomallei* K96243 cells were opsonized by incubating with purified antibodies at various concentrations. Human PMNs were purified by 3% dextran sedimentation T-500 and Ficoll-PaquePLUS centrifugation (Amersham Biosciences). Purified PMNs were cultured to opsonized FITC-labeled bacteria at 37 °C for 30 min, after that 2,800 ng/mL of hydroethidine (HE) (Sigma-Aldrich) was added and incubated for 5 min at 37 °C. Following oxidative burst, HE was metabolized into ethidium bromide (EB), washed twice and fixed with 2% paraformadehyde. Phagocytosis and oxidative burst activities were analyzed by flow cytometry (FACSCalibur; BD Biosciences). Results are represented as % phagocytosis (total % FITC+) and % oxidative burst (% EB + FITC+). The differences between antibody groups were tested by the paired *t* test.

Intracellular bacterial killing assay. Live *B. pseudomallei* K96243 were opsonized with antibodies at various concentrations, as described above. Purified human PMNs at 5×10^5 cells were cultured with opsonized bacteria (multiply of infection; MOI = 10) at 37 °C for 30 min. Then, extracellular bacteria were killed with 250 ug/mL of kanamycin. After washing, infected PMNs were incubated at 37 °C for a further 3 h with 20 μg/mL of kanamycin to maintain additional extracellular bacteria. Finally, PMNs were lyzed and plated on LB agar at various dilutions for the bacterial count. The differences between antibody groups were tested by the paired *t* test.

■ ASSOCIATED CONTENT

Supporting Information

The Supporting Information is available free of charge on the ACS Publications website at DOI: 10.1021/acsinfecdis.5b00118.

Additional figures, synthetic protocols, product characterization, and any other experimental details. (PDF)

■ AUTHOR INFORMATION

Corresponding Authors

*(Alessandro Gori) Tel: +39 02 2850 0039; Fax: +39 02 2890 1239; E-mail: alessandro.gori@icrm.cnr.it.

*(Giorgio Colombo) Tel: +39 02 2850 0031; Fax: +39 02 2890 1239; E-mail: g.colombo@icrm.cnr.it.

Notes

The authors declare no competing financial interest.

■ ACKNOWLEDGMENTS

This project was supported by Fondazione CARIPLO (Progetto Vaccini, contract number 2009-3577), by Bando Regione Lombardia - Fondazione Cariplo 2013, progetto PROVA, ID 42666248 (2013-0349), and by the Italian Ministry of Education and Research, Flagship (PB05) "InterOmics". The authors thank Dr. Marina Cretich for helpful revision.

■ REFERENCES

(1) Xu, Z.-Q., Flavin, M. T., and Flavin, J. (2014) Combating multidrug-resistant Gram-negative bacterial infections. *Expert Opin. Invest. Drugs 23*, 163−82.

(2) Bush, K., Courvalin, P., Dantas, G., Davies, J., Eisenstein, B., Huovinen, P., Jacoby, G. a., Kishony, R., Kreiswirth, B. N., Kutter, E., Lerner, S. a., Levy, S., Lewis, K., Lomovskaya, O., Miller, J. H., Mobashery, S., Piddock, L. J. V., Projan, S., Thomas, C. M., Tomasz, A., Tulkens, P. M., Walsh, T. R., Watson, J. D., Witkowski, J., Witte, W., Wright, G., Yeh, P., and Zgurskaya, H. I. (2011) Tackling antibiotic resistance. *Nat. Rev. Microbiol. 9*, 894−896.

(3) The value of vaccines. *Nat. Rev. Microbiol.* 2008, *6*, 2−2.10.1038/nrmicro1834

(4) Scully, T. (2014) The age of vaccines. *Nature 507*, S2−S3.

(5) Pichenda, K., Nakamura, K., Morita, A., Kizuki, M., Seino, K., and Takano, T. (2012) Non-hospital DOT and early diagnosis of tuberculosis reduce costs while achieving treatment success. *Int. J. Tuberc. Lung Dis. 16*, 828−34.

(6) DeKosky, S. Early intervention is key to successful management of Alzheimer disease. *Alzheimer Dis. Assoc. Disord.* 2003, *17* (Suppl 4), S99−104.10.1097/00002093-200307004-00004

(7) Srivastava, S., Verma, M., and Henson, D. E. (2001) Biomarkers for Early Detection of Colon Cancer. *Clin. Cancer Res. 7*, 1118−1126.

(8) Purcell, A. W., McCluskey, J., and Rossjohn, J. (2007) More than one reason to rethink the use of peptides in vaccine design. *Nat. Rev. Drug Discovery 6*, 404−414.

(9) Gori, A., Longhi, R., Peri, C., and Colombo, G. (2013) Peptides for immunological purposes: Design, strategies and applications. *Amino Acids 45*, 257−268.

(10) Van Regenmortel, M. H. V. (2009) Synthetic Peptide Vaccines and the Search for Neutralization B Cell. *Open Vaccine J. 2*, 33−44.

(11) Li, W., Joshi, M., Singhania, S., Ramsey, K., and Murthy, A. (2014) Peptide Vaccine: Progress and Challenges. *Vaccines 2*, 515−536.

(12) Van Regenmortel, M. H. V. What is a B-cell epitope? In *Methods Mol. Biol.* Schutkowski, M., Reineke, U., Eds.; 2009; Vol. *524*, pp 3−20.

(13) Bennion, B. J., and Daggett, V. (2002) Protein Conformation and Diagnostic Tests: The Prion Protein. *Clin. Chem. 48*, 2105−2114.

DOI: 10.1021/acsinfecdis.5b00118
ACS Infect. Dis. 2016, 2, 221−230

(14) Correia, B. E., Ban, Y.-E. A., Holmes, M. a, Xu, H., Ellingson, K., Kraft, Z., Carrico, C., Boni, E., Sather, D. N., Zenobia, C., Burke, K. Y., Bradley-Hewitt, T., Bruhn-Johannsen, J. F., Kalyuzhniy, O., Baker, D., Strong, R. K., Stamatatos, L., and Schief, W. R. (2010) Computational design of epitope-scaffolds allows induction of antibodies specific for a poorly immunogenic HIV vaccine epitope. *Structure 18*, 1116−1126.
(15) Ofek, G., Guenaga, F. J., Schief, W. R., Skinner, J., and Baker, D. (2010) Elicitation of structure-specific antibodies by epitope scaffolds. *Proc. Natl. Acad. Sci. U. S. A. 107*, 17880−17887.
(16) Azoitei, M. L., Correia, B. E., Ban, Y.-E. A., Carrico, C., Kalyuzhniy, O., Chen, L., Schroeter, A., Huang, P.-S., McLellan, J. S., Kwong, P. D., Baker, D., Strong, R. K., and Schief, W. R. (2011) Computation-guided backbone grafting of a discontinuous motif onto a protein scaffold. *Science (Washington, DC, U. S.) 334*, 373−376.
(17) Timmerman, P., Puijk, W. C., Boshuizen, R. S., Dijken, P. Van, Slootstra, J. W., Beurskens, F. J., Parren, P. W. H. I., Huber, A., Bachmann, M. F., and Meloen, R. H. (2009) Functional Reconstruction of Structurally Complex Epitopes using CLIPS TM Technology. *Open Vaccine J. 2*, 56−67.
(18) Timmerman, P., Puijk, W. C., and Meloen, R. H. (2007) Functional reconstruction and synthetic mimicry of a conformational epitope using CLIPS technology. *J. Mol. Recognit. 20*, 283−299.
(19) Werkhoven, P. R., Van De Langemheen, H., Van Der Wal, S., Kruijtzer, J. a W., and Liskamp, R. M. J. (2014) Versatile convergent synthesis of a three peptide loop containing protein mimic of whooping cough pertactin by successive Cu(I)-catalyzed azide alkyne cycloaddition on an orthogonal alkyne functionalized TAC-scaffold. *J. Pept. Sci. 20*, 235−239.
(20) Misumi, S., Nakayama, D., Kusaba, M., Iiboshi, T., Mukai, R., Tachibana, K., Nakasone, T., Umeda, M., Shibata, H., Endo, M., Takamune, N., and Shoji, S. (2006) Effects of immunization with CCR5-based cycloimmunogen on simian/HIVSF162P3 challenge. *J. Immunol. 176*, 463−471.
(21) Ho, J., Uger, R. A., Zwick, M. B., Luscher, M. A., Barber, B. H., and MacDonald, K. S. (2005) Conformational constraints imposed on a pan-neutralizing HIV-1 antibody epitope result in increased antigenicity but not neutralizing response. *Vaccine 23*, 1559−1573.
(22) Joyce, J. G., Hurni, W. M., Bogusky, M. J., Garsky, V. M., Liang, X., Citron, M. P., Danzeisen, R. C., Miller, M. D., Shiver, J. W., and Keller, P. M. (2002) Enhancement of alpha -helicity in the HIV-1 inhibitory peptide DP178 leads to an increased affinity for human monoclonal antibody 2F5 but does not elicit neutralizing responses in vitro. Implications for vaccine design. *J. Biol. Chem. 277*, 45811−20.
(23) Cromm, P. M., Spiegel, J., and Grossmann, T. N. (2015) Hydrocarbon Stapled Peptides as Modulators of Biological Function. *ACS Chem. Biol. 10*, 1362.
(24) Clark, R. J., Jensen, J., Nevin, S. T., Callaghan, B. P., Adams, D. J., and Craik, D. J. (2010) The engineering of an orally active conotoxin for the treatment of neuropathic pain. *Angew. Chem., Int. Ed. 49*, 6545−8.
(25) Bird, G. H., Irimia, A., Ofek, G., Kwong, P. D., Wilson, I. A., and Walensky, L. D. (2014) Stapled HIV-1 peptides recapitulate antigenic structures and engage broadly neutralizing antibodies. *Nat. Struct. Mol. Biol. 21*, 1058−67.
(26) Verdine, G. L., and Hilinski, G. J. (2012) Stapled peptides for intracellular drug targets. *Methods Enzymol. 503*, 3−33.
(27) Gourlay, L. J., Peri, C., Ferrer-Navarro, M., Conchillo-Solé, O., Gori, A., Rinchai, D., Thomas, R. J., Champion, O. L., Michell, S. L., Kewcharoenwong, C., Nithichanon, A., Lassaux, P., Perletti, L., Longhi, R., Lertmemongkolchai, G., Titball, R. W., Daura, X., Colombo, G., and Bolognesi, M. (2013) Exploiting the burkholderia pseudomallei acute phase antigen BPSL2765 for structure-based epitope discovery/design in structural vaccinology. *Chem. Biol. 20*, 1147−1156.
(28) Peptide stapling techniques based on different macrocyclisation chemistries - c4cs00246f.
(29) Pedersen, D. S., and Abell, A. (2011) 1,2,3-Triazoles in Peptidomimetic Chemistry. *Eur. J. Org. Chem. 2011*, 2399−2411.
(30) Gori, A., Wang, C.-I. A., Harvey, P. J., Rosengren, K. J., Bhola, R. F., Gelmi, M. L., Longhi, R., Christie, M. J., Lewis, R. J., Alewood, P. F., and Brust, A. (2015) Stabilization of the Cysteine-Rich Conotoxin MrIA by Using a 1,2,3-Triazole as a Disulfide Bond Mimetic. *Angew. Chem., Int. Ed. 54*, 1361−4.
(31) Cantel, S., Isaad, A. L. C., Scrima, M., Levy, J. J., DiMarchi, R. D., Rovero, P., Halperin, J. A., D'Ursi, A. M., Papini, A. M., and Chorev, M. (2008) Synthesis and conformational analysis of a cyclic peptide obtained via i to i+4 intramolecular side-chain to side-chain azide-alkyne 1,3-dipolar cycloaddition. *J. Org. Chem. 73*, 5663−74.
(32) Scrima, M., Le Chevalier-Isaad, A., Rovero, P., Papini, A. M., Chorev, M., and D'Ursi, A. M. (2010) Cu I -Catalyzed Azideâ Alkyne Intramolecular i -to-(i + 4) Side-Chain-to-Side-Chain Cyclization Promotes the Formation of Helix-Like Secondary Structures. *Eur. J. Org. Chem. 2010*, 446−457.
(33) Pedersen, S. L., Tofteng, A. P., Malik, L., and Jensen, K. J. (2012) Microwave heating in solid-phase peptide synthesis. *Chem. Soc. Rev. 41*, 1826−44.
(34) Kolb, H. C., Finn, M. G., and Sharpless, K. B. (2001) Click Chemistry: Diverse Chemical Function from a Few Good Reactions. *Angew. Chem., Int. Ed. 40*, 2004−2021.
(35) Tornøe, C. W., Christensen, C., and Meldal, M. (2002) Peptidotriazoles on solid phase: [1,2,3]-triazoles by regiospecific copper(i)-catalyzed 1,3-dipolar cycloadditions of terminal alkynes to azides. *J. Org. Chem. 67*, 3057−64.
(36) Holland-Nell, K., and Meldal, M. (2011) Maintaining biological activity by using triazoles as disulfide bond mimetics. *Angew. Chem., Int. Ed. 50*, 5204−6.
(37) Lassaux, P., Peri, C., Ferrer-Navarro, M., Gourlay, L. J., Gori, A., Conchillo-Solé, O., Rinchai, D., Lertmemongkolchai, G., Longhi, R., Daura, X., Colombo, G., and Bolognesi, M. (2013) A structure-based strategy for epitope discovery in Burkholderia pseudomallei OppA antigen. *Structure 21*, 167−175.
(38) Morra, G.; Potestio, R.; Micheletti, C.; Colombo, G. Corresponding Functional Dynamics across the Hsp90 Chaperone Family: Insights from a Multiscale Analysis of MD Simulations. In *PLoS Comput. Biol.* Livesay, D. R., Ed.; 2012; Vol. *8*, p e1002433.
(39) Meli, M., Gasset, M., and Colombo, G. (2011) Dynamic diagnosis of familial prion diseases supports the β2-α2 loop as a universal interference target. *PLoS One 6*, e19093.
(40) Monticelli, L., Sorin, E. J., Tieleman, D. P., Pande, V. S., and Colombo, G. (2008) Molecular simulation of multistate peptide dynamics: a comparison between microsecond timescale sampling and multiple shorter trajectories. *J. Comput. Chem. 29*, 1740−52.
(41) Cheng, A. C., and Currie, B. J. (2005) Melioidosis: epidemiology, pathophysiology, and management. *Clin. Microbiol. Rev. 18*, 383−416.
(42) Van Regenmortel, M. H. (2001) Antigenicity and immunogenicity of synthetic peptides. *Biologicals 29*, 209−213.
(43) Chen, Y.-H., Yang, J. T., and Chau, K. H. (1974) Determination of the helix and β form of proteins in aqueous solution by circular dichroism. *Biochemistry 13*, 3350−3359.
(44) Case, D. A.; Berryman, J. T.; Betz, R. M.; Cerutti, D. S.; Cheatham, T. E., III; Darden, T. A.; Duke, R. E.; Giese, T. J.; Gohlke, H.; Goetz, A. W.; Homeyer, N.; Izadi, S.; Janowski, P.; Kaus, J.; Kovalenko, A.; Lee, T. S.; LeGrand, S.; Li, P.; Luchko, T.; Luo, R.; Madej, B.; Merz, K. M.; York, D. M.; and Kollman, P. A. *AMBER 2015*; University of San Francisco: 2015.
(45) Wang, J., Wolf, R. M., Caldwell, J. W., Kollman, P. A., and Case, D. A. (2004) Development and testing of a general amber force field. *J. Comput. Chem. 25*, 1157−74.
(46) Jakalian, A., Jack, D. B., and Bayly, C. I. (2002) Fast, efficient generation of high-quality atomic charges. AM1-BCC model: II. Parameterization and validation. *J. Comput. Chem. 23*, 1623−41.
(47) Joosten, R. P., Te Beek, T. a H., Krieger, E., Hekkelman, M. L., Hooft, R. W. W., Schneider, R., Sander, C., and Vriend, G. (2011) A series of PDB related databases for everyday needs. *Nucleic Acids Res. 39*, 411−419.
(48) Kabsch, W., and Sander, C. (1983) Dictionary of protein secondary structure: pattern recognition of hydrogen-bonded and geometrical features. *Biopolymers 22*, 2577−637.

DOI: 10.1021/acsinfecdis.5b00118
ACS Infect. Dis. 2016, 2, 221−230

(49) Vranken, W. F., Boucher, W., Stevens, T. J., Fogh, R. H., Pajon, A., Llinas, M., Ulrich, E. L., Markley, J. L., Ionides, J., and Laue, E. D. (2005) The CCPN data model for NMR spectroscopy: development of a software pipeline. *Proteins: Struct., Funct., Genet. 59*, 687−96.
(50) Wüthrich, K. (1983) Sequential individual resonance assignments in the 1H-nmr spectra of polypeptides and proteins. *Biopolymers 22*, 131−8.
(51) Clark, R. J., Fischer, H., Dempster, L., Daly, N. L., Rosengren, K. J., Nevin, S. T., Meunier, F. A., Adams, D. J., and Craik, D. J. (2005) Engineering stable peptide toxins by means of backbone cyclization: stabilization of the alpha-conotoxin MII. *Proc. Natl. Acad. Sci. U. S. A. 102*, 13767−72.

DOI: 10.1021/acsinfecdis.5b00118
ACS Infect. Dis. 2016, 2, 221−230